Commun. Korean Math. Soc. **22** (2007), No. 4, pp. 623–640

hp-DISCONTINUOUS GALERKIN METHODS FOR THE LOTKA-MCKENDRICK EQUATION: A NUMERICAL STUDY

SHIN-JA JEONG, MI-YOUNG KIM†, AND TSENDANYSH SELENGE

ABSTRACT. The Lotka-McKendrick model which describes the evolution of a single population is developed from the well known Malthus model. In this paper, we introduce the Lotka-McKendrick model. We approximate the solution to the model using *hp*-discontinuous Galerkin finite element method. The numerical results show that the presented *hp*-discontinuous Galerkin method is very efficient in case that the solution has a sharp decay.

1. The Lotka-McKendrick equation

In this paper, we study the Lotka-McKendrick equation and we approximate the solution to the model using *hp*-discontinuous Galerkin finite element methods. Depending on the phenomenon that has to be modelled, the population is given a structure that is often responsible for special behaviors not occurring when the structure is absent, i.e., when the population can be considered homogeneous with respect to the parameters that determine the structure. Age is one of the most natural and important parameters structuring a population. In fact, many internal variables, at the level of the single individual, are strictly depending on the age because different ages mean different reproductions and survival capacities, and also different behaviors. We introduce the age-dependent population model, namely, Lotka-McKendrick equation. The Lotka-McKendrick model which describes the evolution of a single population is developed from the well-known Malthus model. Here, we consider a single population living isolated in an invariant habitat. We assume that all of its individuals are perfectly equal except their age. In particular, we assume that there are no sex differences. In accordance with this phenomenological setting, fertility and mortality are intrinsic parameters of the population growth and do not depend on time, nor on the population size; they are functions of age

Received July 11, 2007.

2000 *Mathematics Subject Classification.* 65M10, 65M20, 92A15, 65C20.

Key words and phrases. age-dependent population dynamics, integro-differential equation, *hp*-discontinuous Galerkin finite element method.

†The research of this author was supported by Inha University Research Grant (INHA-30190).

©2007 The Korean Mathematical Society

only. Let $a_\dagger$ denote the *maximum age* which we assume to be finite. With the premises presented above, the evolution of the population is described by its *age density* function at time t;

$$u(a,t) \; a \in [0, a_\dagger], \; t \geq 0 \, .$$

Thus the integral gives the number of individuals that, at time t, have age in the interval $[a_1, a_2]$; $\int_{a_1}^{a_2} u(a,t)\, da$ and *total population* at time t is

$$P(t) \; = \; \int_0^{a_\dagger} u(a,t)\, da. \tag{1}$$

Concerning *fertility* and *mortality* we first introduce the age specific fertility, $\beta(a)$, which can be defined as the number of newborn, in one time unit, coming from a single individual whose age is in the infinitesimal age interval $[a, a+da]$. Thus $\int_{a_1}^{a_2} \beta(a)u(a,t)\, da$ gives the number of newborn in one time unit, coming from individuals with age in $[a_1, a_2]$. We also consider the *total birth rate*

$$B(t) \; = \; \int_0^{a_\dagger} \beta(a)u(a,t)\, da$$

which gives the total number of newborns in one time unit. We also introduce the *age specific mortality*, $\mu(a)$. It is the death rate of people having age in $[a,a+da]$. Then the *total death rate* is

$$D(t) \; = \; \int_0^{a_\dagger} \mu(a)u(a,t)\, da \tag{2}$$

and it gives the total number of deaths occurring in one time unit. The functions $\beta(\cdot)$ and $\mu(\cdot)$ are, of course, non-negative. They are also called *vital rates* and are viewed as deterministic rates; in practice they are determined on a statistical basis. Other meaningful quantities are derived form $\beta(\cdot)$ and $\mu(\cdot)$,

$$\prod(a) = e^{-\int_0^a \mu(\sigma)d\sigma}, \quad a \in [0, a_\dagger]$$

denotes the *survival probability*, i.e., the probability for an individual to survive to age a.

The Lotka-McKendrick equation is then given as follows [2]:

$$\begin{cases} u_t(a,t) \; + \; u_a(a,t) \; + \; \mu(a)\, u(a,t) \; = \; 0, & 0 < a < a_\dagger, \; t > 0, \\ u(0,t) \; = \; \int_0^{a_\dagger} \beta(\sigma)\, u(\sigma,t)\, d\sigma, & t > 0, \\ u(a,0) \; = \; u_0(a), & 0 \leq a < a_\dagger. \end{cases} \tag{3}$$

Recently, several numerical methods have been proposed to approximate the solution to (3) in case that μ is unbounded. See, for example, [4]-[6] and the references cited therein.

We now list the assumptions that the biological parameters are supposed to fulfill for the biological meaning and/or for the mathematical treatment.

$$\beta(\cdot) \text{ is non-negative and belongs to } L^\infty(0, a_\dagger),$$

$$\mu(\cdot) \text{ is non-negative and belongs to } L^1_{loc}([0, a_\dagger)),$$

$$\int_0^{a_+} \mu(\sigma)\, d\sigma \;=\; +\infty, \tag{4}$$

$$u_0 \;\in\; L^1(0, a_\dagger)\;, \qquad u_0(a) \geq 0, \quad \text{a.e. in } [0, a_\dagger].$$

Condition (4) is necessary for the survival probability $\prod(a)$ to vanish at the age $a_\dagger$.

The organization of the paper is as follows. In section 2, we introduce the *hp*-finite element spaces in one and two dimension. In section 3, we approximate the solution to the model by *hp*-discontinuous Galerkin methods. Finally, in section 4, we show numerical results through several numerical experiments.

2. *hp*-finite element spaces

Most methods for the numerical treatment of partial differential equations are based on approximating the sought solution by piecewise polynomials. Many methods employed today are so called low order methods, in which the underlying polynomial degree p is fixed (typically $p \leq 2$) and convergence is achieved by decreasing the mesh size h. These methods are also called h-methods and have algebraic rates of convergence at best. On the other hand, high order methods such as the p- and *hp*-version finite element methods emerged in the early 1980s. In these methods, the polynomial degree p is increased while still keeping the option to perform mesh refinement. These high order methods are the most appreciated for their high accuracy, for their rates of convergence are often very high and can in certain cases even be exponential. The *hp*-version of finite element method is shown by proper combination of mesh refinement and increasing polynomial degree.

In this section, we shall closely follow [10] and introduce the *hp*-version approximate spaces in one and two dimensions. Let $\Omega = (a, b) \subset \mathbb{R}$ be a bounded interval. A mesh $\mathcal{T}$ on Ω is a partition of Ω into $M(\mathcal{T})$ open, disjoint subintervals $\Omega_j^{\mathcal{T}}$, $\mathcal{T} = \{\Omega_j^{\mathcal{T}}\}_{j=1}^{M(\mathcal{T})}$, $\Omega_j^{\mathcal{T}} = (x_{j-1}^{\mathcal{T}},\ x_j^{\mathcal{T}})$, $a = x_0^{\mathcal{T}} < x_1^{\mathcal{T}} < \cdots < x_M^{\mathcal{T}} = b$. The points $x_j^{\mathcal{T}} \in \overline{\Omega}$ are nodal points and the $\Omega_j^{\mathcal{T}}$ are the elements of the mesh $\mathcal{T}$. Let

$$h_j^{\mathcal{T}} := x_j^{\mathcal{T}} - x_{j-1}^{\mathcal{T}},\ j = 1, \ldots, M,$$

and

$$h(\mathcal{T}) = \max_{1 \leq j \leq M(\mathcal{T})} \{h_j^{\mathcal{T}}\}.$$

Here $h(\mathcal{T})$ is called the meshwidth of $\mathcal{T}$. Each element $\Omega_j^{\mathcal{T}} \in \mathcal{T}$ can be mapped onto $\widehat{\Omega}$=(-1,1), the reference or master element. We denote the map by Q_j, i.e.,

$$\Omega_j = Q_j^{\mathcal{T}}(\widehat{\Omega}),\ x = Q_j(\xi). \tag{5}$$

Evidently, a linear mapping Q_j will suffice for (5)

$$x = Q_j(\xi) = \frac{1}{2}(1-\xi)x_{j-1} + \frac{1}{2}(1+\xi)x_j,\ \xi \in \widehat{\Omega}. \tag{6}$$

Its inverse is

$$\xi = Q_j^{-1}(x) = \frac{2x - x_j - x_{j-1}}{x_j - x_{j-1}},\ x \in \Omega_j.$$

The jacobian of Q_j is constant such that

$$\frac{dx}{d\xi} = \frac{1}{2}(x_j - x_{j-1}) = \frac{h_j}{2}.$$

We now define the global finite element space $S^{\boldsymbol{p},l}(\Omega,\mathcal{T})$ as follows:

Definition 2.1. Let $\boldsymbol{p} = (p_1,\ldots,p_M)$ be a degree vector of polynomial degrees p_j and let $l \geq 0$ be an integer. Let S^p denote the polynomials of degree p on the master element $\widehat{\Omega}$. Then we let

$$S^{\boldsymbol{p},l}(\Omega,\mathcal{T}) = \{u \in H^l(\Omega) : u|_{\Omega_j} = s_j(Q_j^{-1}(x)),\ s_j \in S^{p_j}(\widehat{\Omega})\},$$

where $H^l(\Omega)$ is the standard Sobolev space [10].

Since Q_j is linear, $u \in S^{\boldsymbol{p},l}(\Omega,\mathcal{T})$ implies that on $\Omega_j \in \mathcal{T}$, u is a polynomial of degree p_j. We introduce basis of $S^{\boldsymbol{p},l}(\Omega,\mathcal{T})$ by transporting a basis of $S^{\boldsymbol{p}}$ on $\widehat{\Omega}$ to Ω_j via Q_j. The basis functions of S^p are denoted by $N_i(\xi), i = 1,\ldots,p+1$ and are called standard shape functions. Many different selections of shape functions are possible. We present one, the so-called hierarchic shape functions which are particularly suitable for high polynomial degrees. The selection of shape functions depends also on the degree l of smoothness of $S^{\boldsymbol{p},l}(\Omega,\mathcal{T})$. If $l = 0$, we choose simply the Legendre polynomials

$$N_i(\xi) = L_{i-1}(\xi),\ i = 1,\ldots,p+1.$$

Note that due to the orthogonality of the Legendre polynomials we have

$$\int_{-1}^{1} \frac{dN_i}{d\xi}\frac{dX_j}{d\xi}d\xi = \delta_{ij},\ i,j \geq 3.$$

It is useful to divide the shape functions into 2 sets, internal and external shape functions. We say that $N_i(\xi)$ is an internal shape function of order l, if

$$\frac{d^j N_i}{d\xi^i}(\pm 1) = 0, \qquad 0 \leq j \leq l-1. \tag{7}$$

Shape functions which are not internal are external. For $l = 0$, (7) is void and all shape functions are internal.

We now introduce the space $S^{\boldsymbol{p},l}(\Omega,\mathcal{T})$ in two dimension. Let $\mathcal{T}$ be a triangular mesh in the (straight) polygon $\Omega \subseteq \mathbb{R}^2$. The definition of $S^{\boldsymbol{p},l}(\Omega,\mathcal{T})$ in two-dimension is quite similar to that in the one-dimensional case. Again, functions in $S^{\boldsymbol{p},l}(\Omega,\mathcal{T})$ are, in local coordinates, polynomials of the appropriate degrees. Now, to define the global finite element space $S^{\boldsymbol{p},l}(\Omega,\mathcal{T})$, we associate

each triangle $K \in \mathcal{T}$ with a polynomial degree p_k and combine the elemental polynomial degrees in the degree vector $\boldsymbol{p}$. The definition of $S^{\boldsymbol{p},\,l}(\Omega, \mathcal{T})$ is then given as follows.

Definition 2.2. For an integer $l \geq 0$, define

$$S^{\boldsymbol{p},\,l}(\Omega, \mathcal{T}) = \{u \in H^l(\Omega) : u|_K \in S^{\boldsymbol{p},\,l}(K) \text{ for } K \in \mathcal{T}\}.$$

Of greatest importance are the cases $l = 0$ (discontinuous functions), $l = 1$ (C^0-functions), and $l = 2$ (C^1-functions).

Definition 2.3. A set of points in Ω such that $u \in S^{\boldsymbol{p},\,l}(\Omega, \mathcal{T})$ is (uniquely) determined by its values at these points are called (unisolvent) nodes. Functions $u \in S^{\boldsymbol{p},\,l}$ which are nonzero in exactly one node are called a nodal basis of $S^{\boldsymbol{p},\,l}$.

For the *hp*-discontinuous Galerkin formulation, we need reference elements, namely the reference triangle

$$\begin{aligned}\widehat{K} = \{(\xi,\eta) \in \mathbb{R}^2 : \quad & 0 \leq \eta \leq (1+\xi)\sqrt{3}, \quad -1 \leq \xi \leq 0 \quad \text{or} \\ & 0 \leq \eta \leq (1-\xi)\sqrt{3}, \quad 0 \leq \xi \leq 1\}.\end{aligned}$$

We use the notation $\widehat{K}$ for the generic reference element. Let $\mathcal{T} = \{K_j\}$ be any (regular or irregular) mesh on Ω. With each triangular element K we associate an element mapping

$$Q_j \; : \; \widehat{K} \longrightarrow K_j, \quad K_j \in \mathcal{T}.$$

We define several sets $S_i^{\boldsymbol{p}}$ of polynomials on $\widehat{K}$. We begin with

$$S_1^{\boldsymbol{p}}(\widehat{K}) = \{u^h = \sum_{\substack{0 \leq i,j \leq p \\ i+j \leq p}} c_{ij}\, \xi^i\, \eta^j,\; c_{ij} \in \mathbb{R}, (\xi,\eta) \in \widehat{K}\},$$

the space of polynomials of (total) degree at most p on $\widehat{K}$. Evidently,

$$\dim(S_1^{\boldsymbol{p}}(\widehat{K})) \;=\; \frac{(p+1)(p+2)}{2} \;=\; \frac{p^2}{2} + O(p). \tag{8}$$

Let us now turn to shape functions for $\widehat{K}$. To define hierarchic shape functions on $\widehat{K}$, we introduce barycentric coordinates via

$$\lambda_1 = \frac{1}{2}\left(1 - \xi - \frac{\eta}{\sqrt{3}}\right), \;\; \lambda_2 = \frac{1}{2}\left(1 + \xi - \frac{\eta}{\sqrt{3}}\right), \;\; \lambda_3 = \frac{\eta}{\sqrt{3}}. \tag{9}$$

Evidently,

$$\lambda_1 \;+\; \lambda_2 \;+\; \lambda_3 \;=\; 1.$$

λ_i is equal to one at vertex $\hat{v}_i$ and vanishes on the opposite side $\hat{\gamma}_i$. The hierarchic shape functions on $\widehat{K}$ again consist of the following three groups: First, three nodal shape functions are given by

$$\overset{0}{N}_i\,(\xi,\eta) \;=\; \lambda_i, \quad i \;=\; 1,2,3.$$

Secondly, $p-1$ side shape functions $\overset{1}{N}{}_i^{[j]}(\xi,\eta)$, $i=1,2,\ldots,p-1$, $j=1,2,3$, associated with side $\widehat{\gamma}_j$ of $\widehat{K}$ vanish at the vertices. We construct them only for the side $\widehat{\gamma}_1$, i.e., $\overset{1}{N}{}_i^{[1]}$. Then $\overset{1}{N}{}_i^{[j]}$, $j=2,3$, can be obtained by permutation of indices. To construct $\overset{1}{N}{}_i^{[1]}$, we let $\psi_i(\eta)$ be the normalized antiderivatives of the Legendre polynomials:

$$\psi_i(\eta)=\sqrt{\frac{2i+1}{2}}\int_{-1}^{\eta}L_i(t)dt,\ i=1,2,3,\ldots.$$

We then note that $\psi_i(\pm1)=0$. Write

$$\psi_i(\eta)=\frac{1}{4}(1-\eta^2)\,\varphi_i(\zeta),\ i=1,2,3,\ldots$$

with $\varphi_i(\eta)$ being a polynomial of degree $i-1$. Then the side modes are defined by

$$\overset{1}{N}{}_i^{[1]}(\xi,\eta)=\lambda_2\lambda_3\varphi_i(\lambda_3-\lambda_2),$$

$$\overset{1}{N}{}_i^{[2]}(\xi,\eta)=\lambda_3\lambda_1\varphi_i(\lambda_1-\lambda_3), \tag{10}$$

$$\overset{1}{N}{}_i^{[3]}(\xi,\eta)=\lambda_1\lambda_2\varphi_i(\lambda_2-\lambda_1),\qquad i=1,\ldots,p-1. \tag{11}$$

We note that $\overset{0}{N}{}_i^{[j]}$, $\overset{1}{N}{}_i^{[j]}$, $1\le j\le 3$, $1\le i\le p-1$ are the external shape functions. Finally, in order to construct the third group, which consists of the internal shape functions, let

$$\varepsilon^p(\widehat{K})=\operatorname{span}\{\overset{0}{N}{}_i^{[j]},\overset{1}{N}{}_i^{[j]}:1\le j\le 3,1\le i\le p-1\}$$

and let

$$\mathcal{L}^p(\widehat{K})=\operatorname{span}\{\overset{2}{N}{}_i:\overset{2}{N}{}_i\in(\mathcal{S}_1^p\cap H_0^1)(\widehat{K})\}$$

be the space generated by the internal shape functions $\overset{2}{N}{}_i$. We now note that

$$\begin{aligned}\dim(\mathcal{L}^p(\widehat{K}))&=\dim(\mathcal{S}_1^p(\widehat{K}))-\dim(\varepsilon^p(\widehat{K}))\\&=(p+1)(p+2)/2-(3+3(p-1))\\&=(p-1)(p-2)/2.\end{aligned}$$

Hence, nontrivial internal shape functions on $\widehat{K}$ exist only if $p\ge 3$. Higher-order internal shape functions can be constructed from any basis for $\mathcal{S}_1^p(\widehat{K})$. For $p=3$, there is exactly one internal shape function, the basic bubble function on $\widehat{K}$;

$$b_T(\xi,\eta)=\lambda_1\lambda_2\lambda_3=\frac{\eta}{4\sqrt{3}}\left(\left(1+\frac{\eta}{\sqrt{3}}\right)^2-\xi^2\right). \tag{12}$$

3. *hp*-discontinuous Galerkin approximation

We are now ready to approximate the solution to (3) using *hp*-discontinuous Galerkin methods. Let $\Omega = [0, a_\dagger] \times [0, T]$ be the domain in $\mathbb{R}^2$ with boundary Γ, where $T > 0$ is the final time. Lotka-McKendrick equation (3) can then be rewritten as the following boundary value problem:

$$\begin{aligned} \nu \cdot \nabla u + \tfrac{1}{\sqrt{2}} \mu u &= 0, && \text{in } \Omega, \\ u &= g, && \text{on } \Gamma_-, \end{aligned} \tag{13}$$

where

$$g(a,t) = \begin{cases} \int_0^{a_\dagger} \beta(\sigma) u(\sigma, t) d\sigma, & \text{if } (a,t) \in \Gamma_-^1, \\ u_0(a), & \text{if } (a,t) \in \Gamma_-^2. \end{cases}$$

Here $\nu = (\frac{1}{\sqrt{2}}, \frac{1}{\sqrt{2}})$ and Γ_- is the inflow boundary defined by $\Gamma_- = \{x \in \Gamma : n(x) \cdot \nu < 0\}$, $\Gamma_-^1 = \{(0,t) : 0 \le t \le T\}$, $\Gamma_-^2 = \{(a,0) : 0 \le a \le a_\dagger\}$, and $\Gamma_- = \Gamma_-^1 \cup \Gamma_-^2$. $n(x)$ is the outward unit normal to Γ at the point $x \in \Gamma$. We then notice that the boundary values are prescribed only on the inflow part Γ_-.

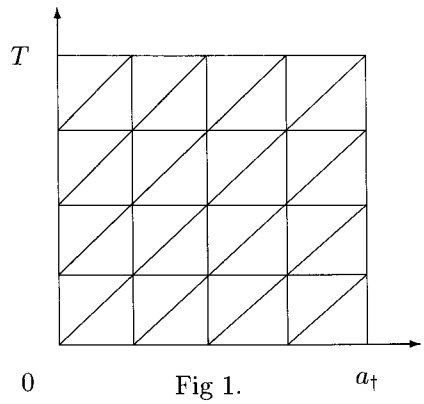

Fig 1.

Now, let $M = \frac{a_\dagger}{h}$, $N = \frac{T}{h}$, where $h = a_i - a_{i-1} = t^j - t^{j-1}$ and let $\mathcal{T}$ be the quasi-uniform triangulation of Ω especially as in Fig 1. For $K \in \mathcal{T}$, we split the boundary ∂K of the triangle K into an inflow part ∂K_- and outflow part ∂K_+

$$\partial K_- = \{x \in \partial K : n(x) \cdot \nu < 0\}, \quad \partial K_+ = \{x \in \partial K : n(x) \cdot \nu \ge 0\}.$$

For function v which may have a jump discontinuity across interelement boundaries, we define the left and right hand limits v_- and v_+ by

$$v_-(x) = \lim_{s \to 0^-} v(x + s\nu), \qquad v_+(x) = \lim_{s \to 0^+} v(x + s\nu),$$

and the jump $[v]$ across interelement boundaries by $[v] = v_+ - v_-$. We shall also use the following notations:

$$\langle v, w\rangle_= \int_\Gamma vwn \cdot \nu \, ds, \quad \langle v, w\rangle_- = \int_{\Gamma_-} vwn \cdot \nu \, ds, \quad \langle v, w\rangle_+ = \int_{\Gamma_+} vwn \cdot \nu \, ds,$$

where $\Gamma_+ = \Gamma \backslash \Gamma_- = \{x \in \Gamma : n(x) \cdot \nu \geq 0\}$, dx denotes the element of area in $\mathbb{R}^2$, and ds the element of arc length along the boundary.

The *hp*-discontinuous Galerkin method for (13) is now written as follows [7]: Find $u^h \in S^{\boldsymbol{p},0}(\Omega, \mathcal{T})$ such that

$$B(u^h, v) = F(v) \quad \text{for all} \quad v \in S^{\boldsymbol{p},0}(\Omega, \mathcal{T}),$$

where

$$B(u^h, v) = \sum_{K \in \mathcal{T}} B^{[K]}(u^h, v), \quad F(v) = - < g, v >_- ,$$

$B^{[K]}(u^h, v)$ is the elemental bilinear form defined by

$$B^{[K]}(u^h, v) = \int_K (\nu \cdot \nabla u^h + \frac{1}{\sqrt{2}} \mu u^h) v \, dx - \int_{\partial K_-} u^h_+ v_+ n \cdot \nu ds.$$

Since $n \cdot \nu = -\frac{1}{\sqrt{2}}$ along the inflow boundary ∂K_- on triangle K ,

$$\begin{aligned} B^{[K]}(u^h, v) &= \int_K (u^h_a + u^h_t + \mu u^h) v \, dx + \int_{\partial K_-} u^h_+ v ds \\ &= \int_{\partial K_-} u^h_- v_+ ds, \quad \forall \, v \in S^{\boldsymbol{p},0}(K). \end{aligned} \tag{14}$$

Now $u^h \in S^{\boldsymbol{p},0}(K)$ has the representation

$$u^h = \sum_{i=1}^{L} x_i T_i, \tag{15}$$

where $L = \frac{(p+1)(p+2)}{2}$ and T_i is the local shape functions appropriate to an L-nodes triangle elements. Hence, substituting (15) into (14) for the case of $v = T_i$, $i = 1, \ldots, L$, we obtain the following linear system of equation:

$$AX = R$$

where $A = (a_{ij})_{L \times L}$ and $R = (r_i)_{L \times 1}$ are given by

$$a_{ij} = \int_K \left(\frac{\partial T_j}{\partial a} + \frac{\partial T_j}{\partial t} \right) T_i \, da \, dt + C_{ij} + D_{ij}, \quad r_i = \int_{\partial K_-} u^h_- T_i \, ds, \tag{16}$$

$$C_{ij} = \int_K \mu(a) T_i \, T_j da \, dt, \quad F_{ij} = \int_K \left(\frac{\partial T_j}{\partial a} + \frac{\partial T_j}{\partial t} \right) T_i \, da \, dt,$$

$$D_{ij} = \begin{cases} \int_{\partial K_-} T_i(a, t^{n-1}) \, T_j(a, t^{n-1}) \, ds, & \text{on } \underline{K}^{\,n}_{\,m}, \\ \int_{\partial K_-} T_i(a_{m-1}, t) \, T_j(a_{m-1}, t) \, ds, & \text{on } \overline{K}^{\,n}_{\,m}. \end{cases}$$

Here $\underline{K}$ and $\overline{K}$ are the typical triangles of $\mathcal{T}$ as shown in Fig 2.

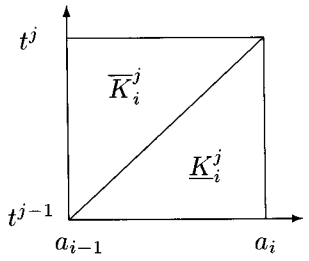

Fig 2.

We here note that the vector R is computed in different way depending on K due to the different form of g in (13). Now, let R_1 and R_2 denote the vector for $\underline{K}_i^j$ corresponding to $j = 1$ and $j \neq 1$, respectively. Also, let R_3 and R_4 denote the vector for $\overline{K}_i^j$ corresponding to $i = 1$ and $i \neq 1$, respectively.

Since we approximate the solution to (13) using discontinuous Galerkin finite element method, we only consider the case of $l = 0$. Namely, we consider

$$S^{\boldsymbol{p},0}(\Omega, \mathcal{T}) = \{u \in H^0(\Omega) : u|_K \in S^{\boldsymbol{p},0}(K) \text{ for } K \in \mathcal{T}\}.$$

For computation in the following section, we consider the following three cases.

Case 1 : The linear case (degree vector $\boldsymbol{p}_j = \mathbf{1}$, $1 \leq j \leq M$).

Standard local shape functions are defined over the reference triangle $\widehat{K}$ with vertices $\widehat{v}_k$, $k = 1, 2, 3$.

$$\widehat{v}_1 = (-1, 0),\ \widehat{v}_2 = (1, 0),\ \widehat{v}_3 = (0, \sqrt{3}).$$

From (9) and (16), we obtain the following:

$$A = \overset{3}{\mathrm{A}} + \Big(C_{ij} + D_{ij}\Big)_{3\times 3}, \quad \text{on } \underline{K},$$

and

$$A = -\overset{3}{\mathrm{A}} + \Big(C_{ij} + D_{ij}\Big)_{3\times 3}, \quad \text{on } \overline{K},$$

where

$$\overset{3}{\mathrm{A}} = \frac{h}{6}\begin{pmatrix} 1 & -1 & 0 \\ 1 & -1 & 0 \\ 1 & -1 & 0 \end{pmatrix}.$$

For $K = \underline{K}_i^j$, we have

$$R_1 = \begin{pmatrix} 0 \\ \int_{\partial K_-} u_0(a)\, T_2\, da \\ \int_{\partial K_-} u_0(a)\, T_3\, da \end{pmatrix}, \qquad R_2 = \begin{pmatrix} 0 \\ \frac{h}{6}(2\alpha + \gamma) \\ \frac{h}{6}(\alpha + 2\gamma) \end{pmatrix},$$

where $\alpha = u^h(a_{i-1}, t^{j-1})|_{\overline{K}_i^{j-1}}$, and $\gamma = u^h(a_i, t^{j-1})|_{\overline{K}_i^{j-1}}$.

For $K = \overline{K}_1^j$, the boundary condition on Γ_-^1 involves the unknown function u^h. We compute $u_-^h(0,t^j)$ on ∂K_- from $\int_0^{a_1} \beta(\sigma)u^h(\sigma,t^j)d\sigma$ by the Trapezoidal rule

$$\mathrm{Tr}(j) = \frac{h}{2-h\beta(0)}\left\{2\sum_{l=1}^{M-1}\beta(a_l)u^h(a_l,t^j)|_{\overline{K}_l^j} + \beta(a_M)u^h(a_M,t^j)|_{\overline{K}_M^j}\right\}.$$

We then have

$$R_3 = \begin{pmatrix} \frac{h}{6}(2\,\mathrm{Tr}(j-1)+\mathrm{Tr}(j)) \\ 0 \\ \frac{h}{6}(\mathrm{Tr}(j-1)+2\,\mathrm{Tr}(j)) \end{pmatrix}, \qquad R_4 = \begin{pmatrix} \frac{h}{6}(2\omega+\delta) \\ 0 \\ \frac{h}{6}(\omega+2\delta) \end{pmatrix},$$

where $\omega = u^h(a_{i-1},t^{j-1})|_{\underline{K}_{i-1}^j}$ and $\delta = u^h(a_{i-1},t^j)|_{\underline{K}_{i-1}^j}$.

Case 2 : The quadratic case (degree vector $\boldsymbol{p}_j = 2,\ 1 \le j \le M$). Standard local shape functions are defined over the reference triangle with vertices $\widehat{v}_k(\ k = 1,2,3)$ and the mid points of all the sides of the triangle, $\widehat{\gamma}_k(\ k = 1,2,3)$ as shown in Fig 3.

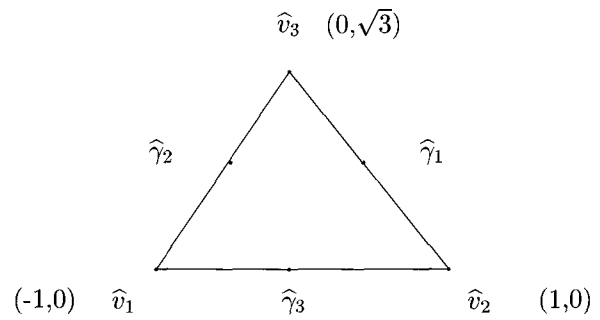

Fig 3.

From (11) and (16), we obtain the following:

$$A = \overset{6}{\mathrm{A}} + \Big(C_{ij} + D_{ij}\Big)_{6\times 6} \text{ on } \underline{K} \quad \text{and} \quad A = -\overset{6}{\mathrm{A}} + \Big(C_{ij} + D_{ij}\Big)_{6\times 6} \text{ on } \overline{K},$$

where

$$\overset{6}{\mathrm{A}} = \begin{pmatrix} \overset{3}{\mathrm{A}} & \overset{3}{\mathrm{B}_1} \\ \overset{3}{\mathrm{B}_2} & \overset{3}{\mathrm{B}_3} \end{pmatrix}_{6\times 6}, \quad \overset{3}{\mathrm{B}_1} = \begin{pmatrix} F_{14} & F_{15} & F_{16} \\ F_{24} & F_{25} & F_{26} \\ F_{34} & F_{35} & F_{36} \end{pmatrix},$$

$$\overset{3}{\mathrm{B}_2} = \begin{pmatrix} F_{41} & F_{42} & F_{43} \\ F_{51} & F_{52} & F_{53} \\ F_{61} & F_{62} & F_{63} \end{pmatrix}, \quad \overset{3}{\mathrm{B}_3} = \begin{pmatrix} F_{44} & F_{45} & F_{46} \\ F_{54} & F_{54} & F_{56} \\ F_{64} & F_{65} & F_{66} \end{pmatrix}.$$

We also see that, for $K = \underline{K}_i^j$,

$$R_1 = \begin{pmatrix} 0 \\ \int_{\partial K_-} u_0(a)\, T_2\, da \\ \int_{\partial K_-} u_0(a)\, T_3\, da \\ \int_{\partial K_-} u_0(a)\, T_4\, da \\ 0 \\ 0 \end{pmatrix}, \qquad R_2 = \begin{pmatrix} 0 \\ \frac{h}{6}(\alpha_1 + 2\alpha_2) \\ \frac{h}{6}(2\alpha_2 + \alpha_3) \\ -\frac{\sqrt{6}h}{60}(\alpha_1 + 8\alpha_2 + \alpha_3) \\ 0 \\ 0 \end{pmatrix},$$

where $\alpha_1 = u^h(a_{i-1}, t^{j-1})|_{\overline{K}_i^{j-1}}$, $\alpha_2 = u^h(a_{i-1} + \frac{h}{2}, t^{j-1})|_{\overline{K}_i^{j-1}}$, and $\alpha_3 = u^h(a_i, t^{j-1})|_{\overline{K}_i^{j-1}}$.

For $K = \overline{K}_1^j$, we compute $u_-^h(0, t^j)$ by Simpson's rule

$$\mathrm{Sp}(j) = \frac{h}{3 - h\beta(0)} \Bigg\{ \beta(a_M) u^h(a_M, t^j)|_{\overline{K}_M^j} + 2 \sum_{l=1}^{\frac{M}{2}-1} \beta(a_{2l}) u^h(a_{2l}, t^j)|_{\overline{K}_{2l}^j} + 4 \sum_{l=1}^{\frac{M}{2}} \beta(a_{2l-1}) u^h(a_{2l-1}, t^j)|_{\overline{K}_{2l-1}^j} \Bigg\}.$$

We thus have

$$R_3 = \begin{pmatrix} \frac{h}{6}(2\,\mathrm{Sp}(j-1) + \mathrm{Sp}(j)) \\ 0 \\ \frac{h}{6}(\mathrm{Sp}(j-1) + 2\,\mathrm{Sp}(j)) \\ 0 \\ -\frac{\sqrt{6}h}{12}(\mathrm{Sp}(j-1) + \mathrm{Sp}(j)) \\ 0 \end{pmatrix}, \qquad R_4 = \begin{pmatrix} \frac{h}{6}(\omega_1 + 2\omega_2) \\ 0 \\ \frac{h}{6}(2\omega_2 + \omega_3) \\ 0 \\ -\frac{\sqrt{6}h}{60}(\omega_1 + 8\omega_2 + \omega_3) \\ 0 \end{pmatrix},$$

where $\omega_1 = u^h(a_{i-1}, t^{j-1})|_{\underline{K}_{i-1}^j}$, $\omega_2 = u^h(a_{i-1} + \frac{h}{2}, t^{j-1})|_{\underline{K}_{i-1}^j}$, and $\omega_3 = u^h(a_{i-1}, t^j)|_{\underline{K}_{i-1}^j}$.

Case 3 : The cubic case (degree vector $\boldsymbol{p}_j = 3,\ 1 \le j \le M$).
Standard local shape functions are defined over the reference triangle with vertices $\widehat{v}_k(\ k = 1, 2, 3)$, the points $\widehat{\gamma}_k(\ k = 1, \ldots, 6)$ of all the sides on the triangle and the center of gravity $\widehat{c}_1$ as shown in Fig 4.

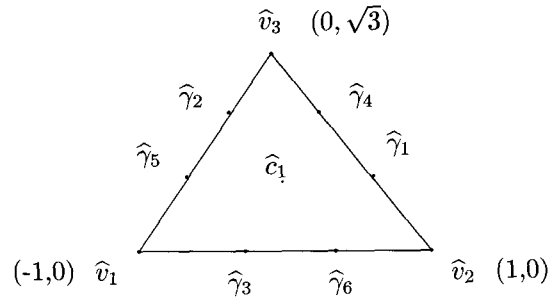

Fig 4.

From (11), (12), and (16), we obtain the following:

$$A = \overset{10}{\mathrm{A}} + \Big(C_{ij} + D_{ij}\Big)_{10\times 10} \text{ on } \underline{K} \text{ and } A = -\overset{10}{\mathrm{A}} + \Big(C_{ij} + D_{ij}\Big)_{10\times 10} \text{ on } \overline{K},$$

where

$$\overset{10}{\mathrm{A}} = \begin{pmatrix} \overset{6}{\mathrm{A}} & \overset{6}{\mathrm{B}}_1 \\ \overset{6}{\mathrm{B}}_2 & \overset{6}{\mathrm{B}}_3 \end{pmatrix},$$

where $\big(\overset{6}{\mathrm{B}}_1\big)_{6\times 4}, \big(\overset{6}{\mathrm{B}}_2\big)_{4\times 6}, \big(\overset{6}{\mathrm{B}}_3\big)_{4\times 4}$,

$$\overset{6}{\mathrm{B}}_1 = \begin{pmatrix} F_{17} & \cdots & F_{1\,10} \\ \vdots & \ddots & \vdots \\ F_{67} & \cdots & F_{6\,10} \end{pmatrix},$$

$$\overset{6}{\mathrm{B}}_2 = \begin{pmatrix} F_{71} & \cdots & F_{76} \\ \vdots & \ddots & \vdots \\ F_{10\,1} & \cdots & F_{10\,6} \end{pmatrix}, \overset{6}{\mathrm{B}}_3 = \begin{pmatrix} F_{77} & \cdots & F_{7\,10} \\ \vdots & \ddots & \vdots \\ F_{10\,7} & \cdots & F_{10\,10} \end{pmatrix}.$$

We also see that, for $K = \underline{K}_i^j$,

$$R_1 = \begin{pmatrix} 0 \\ \int_{\partial K_-} u_0(a)\, T_2\, da \\ \int_{\partial K_-} u_0(a)\, T_3\, da \\ \int_{\partial K_-} u_0(a)\, T_4\, da \\ 0 \\ 0 \\ \int_{\partial K_-} u_0(a)\, T_7\, da \\ 0 \\ 0 \\ 0 \end{pmatrix}, \quad R_2 = \begin{pmatrix} 0 \\ \frac{h}{120}(13\alpha_1 + 36\alpha_2 + 9\alpha_3 + 24\alpha_4) \\ \frac{h}{120}(2\alpha_1 + 9\alpha_2 + 36\alpha_3 + 13\alpha_4) \\ -\frac{\sqrt{6}h}{120}(\alpha_1 + 9\alpha_2 + 9\alpha_3 + \alpha_4) \\ 0 \\ 0 \\ \frac{\sqrt{10}h}{840}(5\alpha_1 + 27\alpha_2 - 27\alpha_3 - 5\alpha_4) \\ 0 \\ 0 \\ 0 \end{pmatrix},$$

where $\alpha_1 = u^h(a_{i-1}, t^{j-1})|_{\overline{K}_i^{j-1}}$, $\alpha_2 = u^h(a_{i-1} + \frac{h}{3}, t^{j-1})|_{\overline{K}_i^{j-1}}$, $\alpha_3 = u^h(a_{i-1} + \frac{2h}{3}, t^{j-1})|_{\overline{K}_i^{j-1}}$, and $\alpha_4 = u^h(a_i, t^{j-1})|_{\overline{K}_i^{j-1}}$.

For $K = \overline{K}_1^j$, i=1, in order to compute $u_-^h(0, t^j)$ we use the Simpson's $\frac{3}{8}$ rule

$$\mathrm{Sn}(j) = \frac{3h}{8 - 3h\beta(0)} \left\{ \beta(a_M) u^h(a_M, t^j)|_{\overline{K}_M^j} + 2 \sum_{l=1}^{\frac{M}{3}-1} \beta(a_{3l}) u^h(a_{3l}, t^j)|_{\overline{K}_{3l}^j} + 3 \sum_{l=1}^{\frac{M}{3}} \left[\beta(a_{3l-1}) u^h(a_{3l-1}, t^j)|_{\overline{K}_{3l-1}^j} + \beta(a_{3l-2}) u^h(a_{3l-2}, t^j)|_{\overline{K}_{3l-2}^j} \right] \right\}.$$

We then have

$$R_3 = \begin{pmatrix} \frac{h}{6}(2\,\mathrm{Sp}(j-1) + \mathrm{Sp}(j)) \\ 0 \\ \frac{h}{6}(\mathrm{Sp}(j-1) + 2\,\mathrm{Sp}(j)) \\ 0 \\ -\frac{\sqrt{6}h}{12}(\mathrm{Sp}(j-1) + \mathrm{Sp}(j)) \\ 0 \\ 0 \\ \frac{\sqrt{10}h}{60}(\mathrm{Sp}(j) - \mathrm{Sp}(j-1)) \\ 0 \\ 0 \end{pmatrix}, \quad R_4 = \begin{pmatrix} \frac{h}{120}(\omega_1 + 36\omega_2 + 9\omega_3 + 2\omega_4) \\ 0 \\ \frac{h}{120}(2\omega_1 + 9\omega_2 + 36\omega_3 + 13\omega_4) \\ 0 \\ -\frac{\sqrt{6}h}{120}(\omega_1 + 9\omega_2 + 9\omega_3 + \omega_4) \\ 0 \\ 0 \\ -\frac{\sqrt{10}h}{840}(5\omega_1 + 27\omega_2 - 27\omega_3 - 5\omega_4) \\ 0 \\ 0 \end{pmatrix},$$

where $\omega_1 = u^h(a_{i-1}, t^{j-1})|_{\underline{K}_{i-1}^j}$, $\omega_2 = u^h(a_{i-1} + \frac{h}{3}, t^{j-1})|_{\underline{K}_{i-1}^j}$, $\omega_3 = u^h(a_{i-1} + \frac{2h}{3}, t^{j-1})|_{\underline{K}_{i-1}^j}$, and $\omega_4 = u^h(a_{i-1}, t^j)|_{\underline{K}_{i-1}^j}$.

We compute u^h in order given in Fig 5.

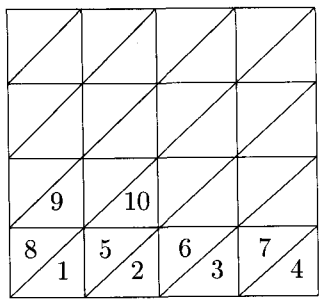

Fig 5. Numbering of triangulation.

That is, we first compute u^h on $\underline{K}_i^1$ for i=1,..., M. Secondly, we compute u^h on $\underline{K}_i^1$ for i=2,..., M. Finally, we compute u^h on $\overline{K}_1^1$ using R_3 which is computed in the previous step.

4. Numerical results

In this section we present some numerical results. We compute the L_2-norm error given by

$$\text{Err} = \|u(\cdot,\cdot) - u^h(\cdot,\cdot)\|_{L_2(\Omega)},$$

where $u(\cdot,\cdot)$ denotes exact solution and u^h approximate solution.

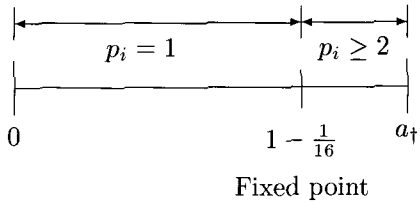

Fig 6. Degree vector $\boldsymbol{p} = (p_1, \ldots, p_i, \ldots, p_M)$ for age.

Example 4.1. We solve problem (13) with the following data:

$$\mu = \frac{1/16}{(1-a)}, \ \beta = \frac{1}{\int_0^{a_\dagger} e^{-x}(1-x)^{1/16}dx},$$

$a_\dagger = 1$, $T = 3$, and $u_0(a) = (1-a)^{1/16}e^{-a}$.

The exact solution is then given by $u(a,t) = u_0(a)\, e^t$.

In Example 4.1, we compared the errors and the elapsed times for different degree vectors $\boldsymbol{p}$ and meshes as given in Fig. 6. The results are given in Tables 1-3 and Fig. 7-11. They showed that the hp-discontinuous Galerkin method is more efficient than the (h-version) discontinuous Galerkin method.

h	$\sharp(p_i \geq 2)$	Linear	Quadratic	Cubic
1/4	1	3.0509470	0.9602459	0.5952960
1/8	1	1.6673910	0.5888727	0.3786952
1/16	1	0.9063975	0.3518454	0.2234626
1/32	2	0.5046173	0.2142716	0.1362357
1/64	4	0.2705931	0.1576934	0.0799887

Table 1. Global L_2 errors for the hp-DG. ($\sharp(l)$ denotes the number of l)

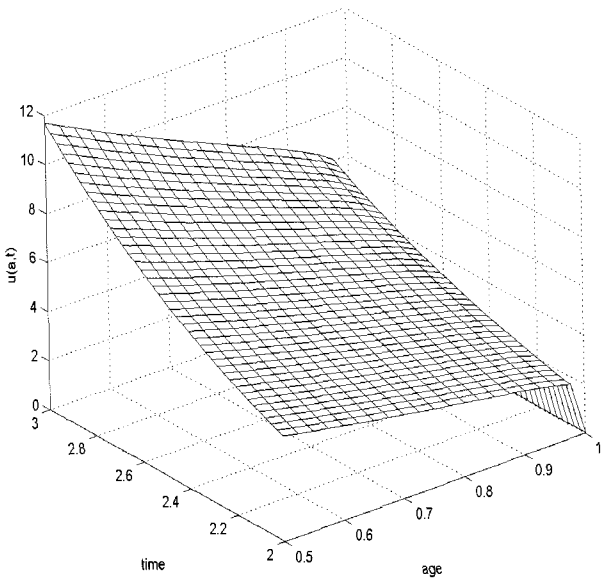

Fig 7. Exact solution $u(a,t) = (1-a)^{1/16}e^{t-a}$.

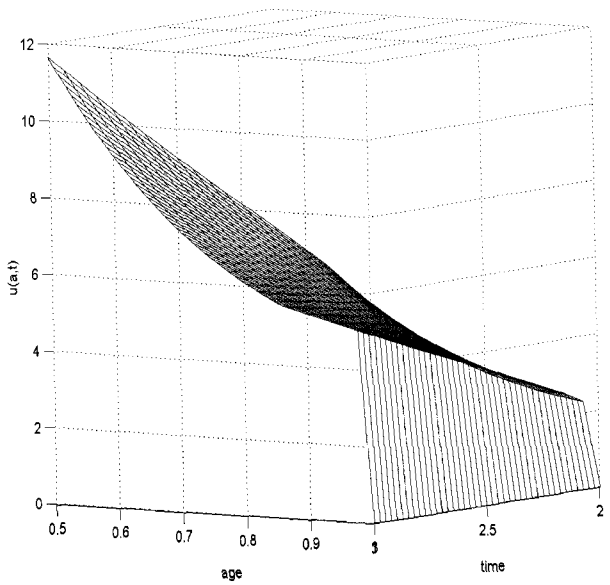

Fig 8. Rotated exact solution of Fig 7.

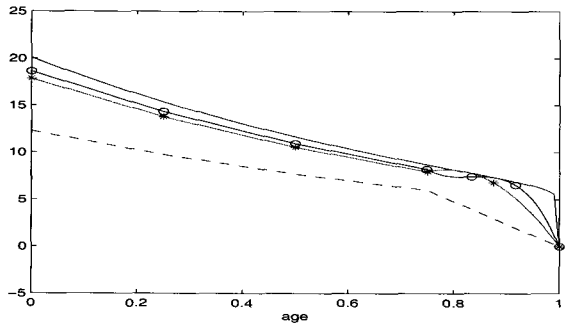

Fig 9. T=3, M=4 and N=12.

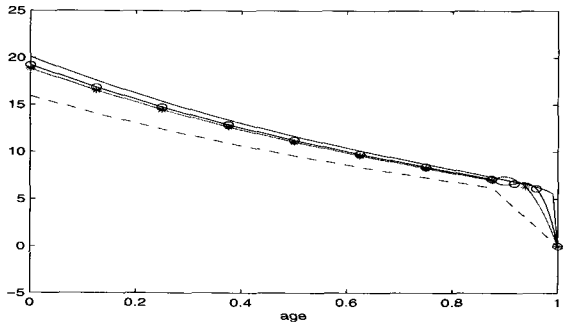

Fig 10. T=3, M=8 and N=24.

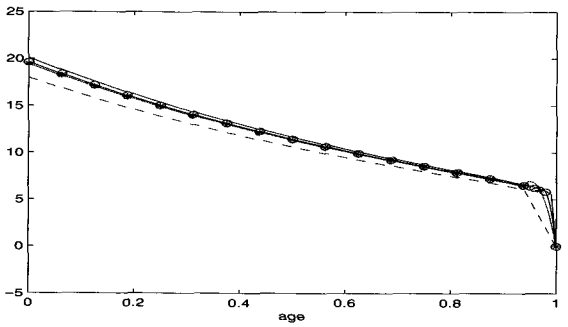

Fig 11. T=3, M=16 and N=48.

— : exact solution at T=3,
- - : approximate solution for degree vector $\boldsymbol{p} = (1, 1, \cdots, 1, 1)$,
* : approximate solution for degree vector $\boldsymbol{p} = (1, 1, \cdots, 1, 2)$,
o : approximate solution for degree vector $\boldsymbol{p} = (1, 1, \cdots, 1, 3)$.

h	$\sharp(p_i \geq 2)$	Linear	Quadratic	Cubic
1/4	1	1.4244180	0.6266852	0.3730726
1/8	1	0.8369876	0.4066835	0.2363213
1/16	1	0.5327252	0.2702307	0.1542003
1/32	2	0.3515174	0.1815984	0.1067758
1/64	4	0.2347559	0.1301275	0.0697881

Table 2. Local L_2 errors for the hp-DG.

L2 - Error	degree vector $\boldsymbol{p}$	h	Elapsed times(sec)
0.2347559	$\boldsymbol{p} = (1, 1, \ldots, 1, 1, 1)$	1/64	3790.009
0.2702307	$\boldsymbol{p} = (1, 1, \ldots, 1, 1, 2)$	1/16	250.2250
0.2363213	$\boldsymbol{p} = (1, 1, \ldots, 1, 1, 3)$	1/8	142.1108

Table 3. Degree vector $\boldsymbol{p}$, mesh size h and the elapsed times when the local L_2-errors are almost same.

It is noted that if the graded mesh is used in triangulation, the oscillations in Fig. 9-11 will be disappeared even with reasonable degree of freedom [11].

References

[1] M. B. Allen and E. L. Isaacson, *Numerical Analysis for Applied Science*, John Wiley & Sons, 1998.

[2] M. Iannelli, *Mathematical Theory of Age-Structured Population Dynamics*, Giardini Editori E Stampatori In Pisa, 1994.

[3] C. Johnson, *Numerical Solution of Partial Differential Equations by the Finite Element Method*, The Cambridge University Press, 1987.

[4] M.-Y. Kim, *A collocation method for the Gurtin–MacCamy equation with finite life-span*, SIAM J. Numer. Anal. **39** (2002), no. 6, 1914–1937.

[5] ———, *Discontinuous Galerkin methods for a model of population dynamics with unbounded mortality*, SIAM J. Sci. Comput. **27** (2006), no. 4, 1371–1393.

[6] ———, *Discontinuous Galerkin methods for the Lotka-Mckendrick equation with finite life-span*, Math. Models Methods Appl. Sci. **16** (2006), no. 2, 161–176.

[7] M.-Y. Kim and Ts. Selenge, *Age-Time Discontinuous Method for the Lotka-McKendrick Equation*, Commun. Korean Math. Soc. **18** (2003), no. 3, 569–580.

[8] P. E. Lewis and J. P. Ward, *The Finite Element Method*, Addison-Wesley Publishing Company, 1991.

[9] J. H. Mathewsm and K. D. Fink, *Numerical Methods using Matlab*, Prentice-Hall, 1999.

[10] M. Melenk, *hp-Finite Element Methods for Singular Perturbations*, Springer, 2002.

[11] Ch. Schwab, *p- and hp-Finite Element Methods: Theory and Applications in Solid and Fluid Mechanics*, Oxford University Press Inc., 1998.

[12] V. Thomee, *Galerkin Finite Element Methods for Parabolic Problems*, Springer Series in Computational Mathematics, Springer, 1997.

Shin-Ja Jeong
Department of Mathematics
Inha University
Incheon 402-751, Korea
E-mail address: sj_0213@inhaian.net

Mi-Young Kim
Department of Mathematics
Inha University
Incheon 402-751, Korea
E-mail address: mikim@inha.ac.kr

Tsendanysh Selenge
Department of Mathematics
Inha University
Incheon 402-751, Korea